J. King Saud Univ., Vol. 11, *Eng. Sci.*(1), pp.85-116 (A.H. 1419/1999)

Interaction between Finite Planar Cracks

Ismail Demir
Mechanical Engineering Department, College of Engineering, King Saud University, P.O. Box 800, Riyadh 11421, Saudi Arabia

(Received 16 March 1997 ; accepted for publication 9 March 1998)

Abstract. Finite cracks located in an infinite planar domain subjected to a given inplane remote loading are considered. The formulation is based on well known dislocation density distribution modeling. General formulation is presented on two interacting cracks and results are also obtained for this case. The effect of the relative positions, orientations and lengths of the cracks on the stress intensity factors and the stress field are analyzed extensively in order to emphasize some of the features which have not been pointed out in previous studies such as. dependence of the shielding regions and the neutral angles on relative crack lengths. influence of the relative crack orientations on the effective crack modes.

In addition to correcting or completing some features in previous studies, applicability of superdislocation model in the crack interaction problems is also investigated. Ground work for representing Peach Koehler force on a dislocation in the stress field of interacting cracks is completed and the close similarity between the stress field of the interacting cracks and their equivalent superdislocation representations is presented. Moreover the stress intensity factors found using the exact solution and approximate superdislocation model are compared and a close similarity is observed. The presented results for some sample cases indicate that superdislocations can represent cracks, however in order to asses exact quantitative accuracy further analysis considering all possible options is required.

Nomenclature

B_{jk}	Strength of a superdislocation
F_k	Peach-Koehler force on a dislocation
K_I,K_{II}	Mode I and II stress intensity factors
S_j	The position of superdislocation
X_L	Horizontal distance of the center of crack 2
Y_L	Vertical distance of the center of crack 2
a_1,a_2	Half lengths of crack 1 and crack 2 respectively
b_1,b_2	Climb and glide components of Burgers vectors of a dislocation respectively

d	Distance from the right tip of crack 1 to the center of crack 2.
α_c	Angle defining the orientation of crack 2
$\delta_{(I)},\delta_{(II)}$	Opening and sliding mode crack face displacements
r,θ	Polar coordinates
μ	Shear modulus
ν	Poisson's ratio
ξ_i	Components of the vector along dislocation line
ρ	The ratio of crack lengths
$\sigma_\infty,\tau_\infty$	Remote external distributed loads
$\sigma_{rr},\sigma_{r\theta},\sigma_{\theta\theta}$	Stress components in polar coordinates

Introduction

Interaction among cracks and some other defects have been studied extensively over the years. The main reason for that is the importance of the subject in understanding the mechanics of failure and developing methods to predict and prevent that. Especially increasing usage of some traditionally brittle materials such as ceramics and the dependence of their fracture toughness on interacting cracks make the subject more attractive. Main effort in the area has been on the interaction between a main crack and finite micro-cracks [1;2] and semi-infinite crack and micro-cracks or flat inclusions [3;4], and other defects [5;6], where the main concern had been the changes in the mode I stress intensity factor of the main crack. The effects of the orientations and locations of the micro-defects or cracks have been investigated extensively in these studies. Approximate closed form solutions for the stress intensity factors of the main crack are obtained as a result of formulation based on complex stress potentials of Muskhelishvili in [2] and [6]. The formulations in [3-5] are based on the dislocation density distribution and treated multiple micro-cracks as well as voids and inclusions ahead of a main semi-infinite crack.

One of the cracks is considered infinite or semi-infinite in most of the previous research works except a few studies such as [7]. Infinite or semi-infinite crack assumptions are mainly due to the fact that, in general, some micro-cracks interact with a much larger main crack in practice. As a result of increasing usage of unconventional materials such as ceramics and composites, in engineering, there have been numerous articles on the subject of crack interaction dealing with the interacting cracks in brittle or inhomogeneous medium [8-10]. Some recent studies on the subject such as [11-14], dealing with further aspects of crack interaction, crack closure, application of numerical techniques and interacting cracks with different shapes indicate the continuing interest on the subject among the researchers.

In order to make the analysis complete and to prevent some misjudgments about previously reported crack shielding zones and to emphasize the effects of finiteness the present analysis is carried out. The first part is devoted to the formulation of the problem. After presentation of the formulation, solution techniques are described and two different approaches are mentioned. Their advantages and disadvantages are briefly discussed. The present formulation first covers the case of interaction of two finite cracks in an infinite planar domain. Extending the problem for multiple cracks becomes a straightforward task after the main formulation is clearly stated. The entire stress field can also be obtained by the present formulation. This provides a powerful tool for the further analysis of crack propagation directions and forces created on dislocations among interacting cracks, their ensuing motion and interlocking positions. The present dislocation formulation makes it possible to represent the extended stress field by pairs of superdislocations. The superdislocation concept and its representation is investigated in the second part. After a brief introduction to the concept, the methods of expressing equivalent strengths and positions of the superdislocations are explained.

The results are presented and discussed later. Definition of the boundaries of shielding and amplification zones is reconsidered for finite cracks. The effect of the relative positions, lengths and orientations of the cracks on the stress intensity factors are discussed. The similarities between the extended stress fields of cracks and representative superdislocations are shown in a given configuration as an example. Furthermore stress intensity factors are calculated using the relation between the force on a dislocation, energy release rate and stress intensity factors in the case of superdislocation representation and compared with the exact solution for the crack case in a couple of sample locations and orientations. The conclusions based on the points raised in the paper, cited in the last section to summarize the main outline of the present work.

Formulation of the Problem

Two finite cracks located in an infinite planar domain are considered first. Increasing the number of cracks will be a simple task once the basic formulation is clarified for two cracks only. As seen in Fig. 1 the two cracks are arbitrarily located relative to each other. The loading is applied at infinity and can be in any orientation. Each crack is represented by the distributions of dislocation densities composed of two components of the Burgers vectors corresponding mode I and mode II. By extending the expressions of [15] for a single edge dislocation the stress field due to a single dislocation made of climb and glide components is given in polar coordinates as follows :

$$\sigma_{rr} = -Db_1 \frac{\cos\theta}{r} + Db_2 \frac{\sin 0}{r},$$
$$\sigma_{\theta\theta} = -Db_1 \frac{\cos\theta}{r} + Db_2 \frac{\sin\theta}{r}, \qquad (1)$$
$$\sigma_{r0} = -Db_1 \frac{\sin\theta}{r} - Db_2 \frac{\sin\theta}{r},$$

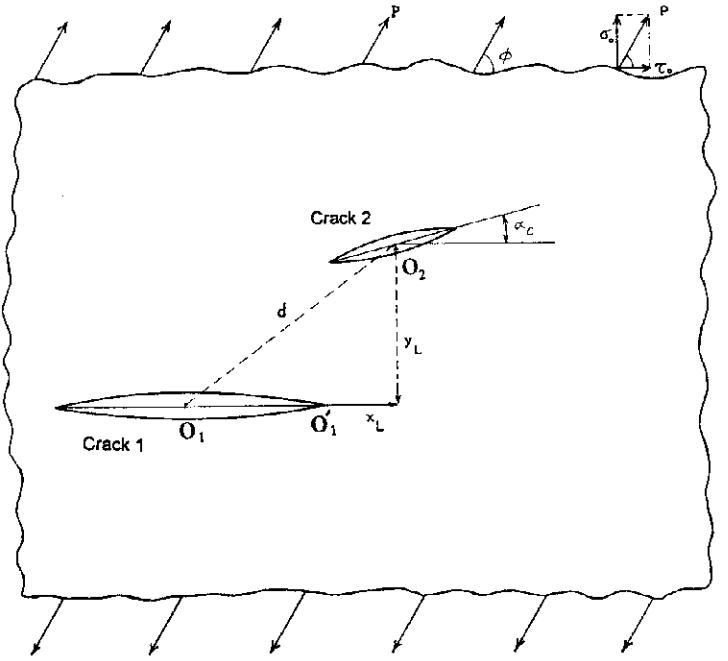

Fig. 1. Two interacting cracks in a uniaxially loaded infinite domain.

where r and θ are polar coordinates, $b_1 = u_{\theta_{0=0}} - u_{\theta_{\theta=2\pi}}$ and $b_2 = u_{r_{\theta=0}} - u_{r_{\theta=2\pi}}$ are climb and glide components of the Burgers vector of a dislocation located at the origin, u_θ, u_r are components of displacements. The factor D which includes shear modulus μ

and Poisson's ratio is expressed as $D = \frac{2\mu}{\pi(\kappa + 1)}$ where $\kappa = 3-4\nu$ for plane strain, $\kappa = (4 - \nu)/(1 + \nu)$ for plane stress.

Using the basic expressions for a single dislocation as Green's function the stress field created by continuous distributions of dislocation densities which are used to represent a crack under the effect of tractions applied to the crack surfaces can be expressed as follows,

$$-D\int_{-a_1}^{a_1} \frac{b_1(s)}{(x-s)}ds = -\sigma_0$$

$$-D\int_{-a_1}^{a_1} \frac{b_2(s)}{(x-s)}ds = -\tau_0 \qquad (2)$$

where a_1 is the half length of the crack, $\theta = 0$ and x axis of the cartesian coordinate is chosen along the crack ($x \equiv r$). The terms on the right hand side σ_0 and τ_0 show the normal and tangential components of the external distributed load acting at infinity which is represented as normal and tangential tractions along the crack faces as a first part of the well known superposition technique. In the case of a single crack the above integral equation can be solved analytically, because the right hand side is simple. On the other hand for the more complicated case of multiple crack interaction it is hard to find an analytical solution even for the case of simple uniaxial loading. Therefore well developed numerical techniques must be used in the solution process.

Let us now consider two arbitrarily oriented finite cracks in an infinite plane which is subjected to inplane loading as seen in Fig. 1 The two cracks are modeled by distribution of dislocation densities representing opening and sliding of crack surfaces relative to each other. The first approach which is used here is the iteration technique. This straightforward method can be outlined as follows

(i) Write all the parameters in equation (2) for crack 1 when crack faces are subjected to internal normal and tangential tractions (i.e. σ_0 and τ_0) equal and opposite to the stresses created by the external loading at infinity. Solution of this integral equation gives the dislocation density distributions for crack 1. Then integrating this distribution obtain the stress field in the presence of only crack 1 as a part of superposition process. As a result of this step the entire stress field will be known as well as the stresses at the location of the second crack.

(ii) Apply the opposite of above stresses found at the location of crack 2 to the faces of this crack considering crack 1 as absent, find the dislocation density distribution for crack 2 and obtain entire stress field, including the location of the crack 1.

(iii) Apply the opposite of these stresses along the surfaces of crack 1 and obtain the entire stress field in the absence of crack 2.

Above steps complete one cycle of the iteration. When this process is repeated, the total stresses and dislocation density distributions converge to a certain value and the iteration will be stopped after a predetermined convergence criteria is met. This technique has been used in some previous studies such as [14;16], however the iteration process is time consuming and it gets more tedious in the case of multiple cracks. This method applied partially in the present study for the purpose of comparison with the coupled integral equation technique. Since the numerical results of both technique are close and accurate as long as the number of iterations is high and the size of divisions along the cracks are fine enough, the comparison basically is made to check the computational effectiveness during the calculations. No more detail is needed about the results of the iteration technique because it will be a repetition of almost the same numbers obtained from the direct solution. The coupled solution is a direct technique which is based on obtaining coupled integral equations from crack 1 and 2 (up to crack n if more cracks are interacting) and solving them simultaneously. After developing the solution independently, close similarities are observed later with the present technique and the method used by Lam and Wen in [3;4]. Although they also used dislocation densities, restricting the formulation to the interaction of semi-infinite crack and microcracks is found to be unnecessary and complete solution for the case of all finite cracks is presented here. This direct method is formulated in the following lines.

Let the dislocation density distributions be b_1, b_2 for crack 1 and b_3, b_4 for crack 2 corresponding to the derivatives of opening and sliding of the crack surfaces respectively. Two pairs of coupled integral equations each corresponding to one of the cracks can be written as follows

$$-D\int_{-a_1}^{a_1} \frac{b_1(s_1)}{(x_1-s_1)}ds_1 = -\sigma_0 + D\int_{-a_2}^{a_2} \left[b_3(s_2)K_{13}(s_2,x_1) + b_4(s_2)K_{14}(s_2,x_1)\right]ds_2 \quad (3)$$

$$-D\int_{-a_1}^{a_1} \frac{b_2(s_1)}{(x_1-s_1)}ds_1 = -\tau_0 + D\int_{-a_2}^{a_2} \left[b_3(s_2)K_{23}(s_2,x_1) + b_4(s_2)K_{24}(s_2,x_1)\right]ds_2 \quad (4)$$

$$-D\int_{-a_2}^{a_1} \frac{b_3(s_2)}{(x_2-s_2)}ds_2 = -\sigma_0' + D\int_{-a_1}^{a_1} \left[b_1(s_1)K_{31}(s_1,x_2) + b_2(s_1)K_{32}(s_1,x_2)\right]ds_1 \quad (5)$$

$$-D\int_{-a_2}^{a_1}\frac{b_4(s_2)}{(x_2-s_2)}ds_2=-\tau_0'+D\int_{-a_1}^{a_1}\left[b_1(s_1)K_{41}(s_1,x_2)+b_2(s_1)K_{42}(s_1,x_2)\right]ds_1 \quad (6)$$

and additional four equations come from the crack closure conditions are

$$\int_{-a_i}^{a_i} b_j(s_i)ds_i=0 \qquad i=1,2 \qquad j=1...4 \quad (7)$$

where kernels K_{ij} are functions of the relative positions of the cracks and the transformation angle of the stresses. The exact forms of these kernels are presented in Appendix A. a_1 and a_2 are the half lengths of crack 1 and 2 respectively. As described before, σ_0 and τ_0 are the normal and tangential components of the external loading along the crack 1 and σ_0' and τ_0' are also similar components along the crack 2 which have the following form

$$\begin{aligned}-\sigma_0' &= -\sigma_0\cos^2\alpha_c-\tau_0\sin 2\alpha_c,\\ -\tau_0' &= -0.5\sigma_0\sin 2\alpha_c+\tau_0\cos 2\alpha_c.\end{aligned} \quad (8)$$

Above integrals are scaled using related crack half-length so that the limits are always -1 to 1. These equations can be discretized and solved by using one of the available techniques after the dislocation density distributions are separated to the singular and the regular parts as $b(s)=\frac{B(s)}{\sqrt{1-s^2}}$. In the present work the Chebyshev polynomial technique as proposed by Erdogan [17], among other techniques, is preferred due to its simplicity. The final forms of the discretized equations are given as

$$\sum_{k=1}^{n}\frac{\overline{B}_1(s_{1k})}{(x_{1r}-s_{1k})}+\overline{B}_3(s_{2k})K_{13}(s_{2k},\hat{x}_{1r})+\overline{B}_4(s_{2k})K_{14}(s_{2k},\hat{x}_{1r})=-\frac{\pi}{n} \quad (9)$$

$$\sum_{k=1}^{n}\frac{\overline{B}_2(s_{1k})}{(x_{1r}-s_{1k})}+\overline{B}_3(s_{2k})K_{23}(s_{2k},\hat{x}_{1r})+\overline{B}_4(s_{2k})K_{24}(s_{2k},\hat{x}_{1r})=\frac{\pi}{n}\overline{\tau}_0 \quad (10)$$

$$\sum_{k=1}^{n} \frac{\overline{B}_3(s_{2k})}{(x_{2r}-s_{2k})} + \overline{B}_1(s_{1k})K_{31}(s_{1k},\hat{x}_{2r}) + \overline{B}_2(s_{1k})K_{32}(s_{1k},\hat{x}_{2r}) = \frac{\pi}{n}\overline{\sigma}'_0 \qquad (11)$$

$$\sum_{k=1}^{n} \frac{\overline{B}_4(s_{2k})}{(x_{2r}-s_{2k})} + \overline{B}_1(s_{1k})K_{41}(s_{1k},\hat{x}_{2r}) + \overline{B}_2(s_{1k})K_{42}(s_{1k},\hat{x}_{2r}) = \frac{\pi}{n}\overline{\tau}'_0 \qquad (12)$$

where $\overline{B}_i = \frac{D}{\sigma_0}B_i$, $\overline{\tau}_0 = \frac{\tau_0}{\sigma_0}$, $\overline{\sigma}'_0 = \frac{\sigma'}{\sigma_0}$ and $\overline{\tau}'_0 = \frac{\tau'_0}{\sigma_0}$, s_k's and x_r's are zeros of Chebyshev polynomials of the first and second type respectively. Indices 1 and 2 beside k and r indicate whether these points are along crack 1 or 2. However their numerical values are the same. $\hat{x}_r$'s are the scaled forms arranged accordingly when changes needed between local and global coordinates to keep the integral boundaries always between -1 and 1 for both cracks. This is needed in order to apply the Chebyshev polynomial technique when the crack lengths are different. Additional four equations are the discretized forms of closure condition which can be written as

$$\sum_{k=1}^{n} \overline{B}_i(s_k) = 0 \qquad i = 1,2,3,4 \qquad (13)$$

Above expressions result in 4N×4N linear systems of equations when both cracks are discretized to N nodes. Solution of above equations gives the dislocation density distribution along both cracks. Crack opening displacements, stress intensity factors, and the entire stress field can be obtained by using these distributions. Moreover each crack can be approximately represented as pairs of superdislocations.

It should be noted here that in the case of multiple crack interaction the basic formulation is the same and only the number of above equations will increase by two for each crack. For instance there will be 2M coupled integral equations for the case of M interacting cracks. The solution technique would still be efficiently applied. When the size of the final form of the linear systems of equations which will be (2M)N ×(2M)N is considered the cost of numerical solution must be taken into consideration and the linear solver to be used must be carefully chosen. Whenever the matrix size becomes a real problem in terms of computation it is still possible to go back to the previously mentioned iteration technique where the size of the linear system would still be (2N×2N) at each step, however it will take much longer time until the convergence criterion is met. Since in the case of too many interacting cracks iteration technique could be preferable to avoid the problems due to the huge size of the matrix this method

mentioned briefly as an alternative and detailed results about the accuracy of the method considered unnecessary to report. Iteration technique takes longer time to converge in general and convergence criteria can be affected by the roundoff errors. The final matrix in the linear system is not a diagonal one and mostly populated making it difficult to deal with when the size is really large (i.e. the case of multiple cracks). In the present study the results are presented for the interaction of two finite cracks. Therefore direct method is used comfortably. The author felt that it is necessary to mention about an alternative method, namely iteration technique, to show how to avoid problems due to large matrix size whenever it would arise. Especially a solution accessible by everyone even for the case of too many interacting cracks by using today's wide spread personal computers, had to be mentioned in order to point out the common and easy applicability of the solution using present formulation.

Crack opening displacements

Crack opening displacement which practically means the gap between the two surfaces of crack due to mode I effect and the amount of shift between the two surfaces of the cracks due to mode II effect at any point x along the cracks can be written immediately, recalling the definition of dislocation density, as follows

$$\delta_{(I)}(x) - \int_{-1}^{x} b_i(s)ds$$

$$\delta_{(II)}(x) == \int_{-1}^{x} b_j(s)ds \qquad (14)$$

where δ is total crack opening displacement (C.O.D.) at x. i shows 1 and 3, and j shows 2 and 4 for crack 1 and 2 respectively.

Stress intensity factors

Using the commonly accepted definition the stress intensity factors can be written as follows

$$K_I = \lim_{x \to (\pm a)} \sqrt{2\pi\left[x - (\pm a)\right]}\sigma_{yy}(x,0)$$

$$K_{II} = \lim_{x \to (\pm a)} \sqrt{2\pi\left[x - (\pm a)\right]}\sigma_{xy}(x,0) \qquad (15)$$

The normalized stress intensity factors can easily be obtained from the dislocation density distributions and given as follows

$$K_I = \pi B_i(\pm a_k), \qquad K_{II} = \pi B_j(+a_k), \tag{16}$$

where i and j are defined in the same way mentioned in (13) and a corresponds to a_1 or a_2 depending on which crack the stress intensity factor belongs to and ± sign is kept there to choose between the right or left tip of the cracks. It is clear from the Fig. 1 that (-) sign always refers to the left hand side tip of the crack while (+) sign refers to the right as long as the relative orientation angle of crack 2 is between 0 and 90 degrees. The stress intensity factors are normalized by $K_I = \sigma_0\sqrt{\pi a_1}$ which is the stress intensity factor of crack 1 if it were alone in the same applied loading condition. In order to make the presentation of results more convenient the following notation for the normalized stress intensity factors is adopted:

$K_{I_{R1}}$: Mode I stress intensity factor for crack 1 at the close (right) tip, ($s_1 = a_1$)

$K_{II_{R1}}$: Mode II stress intensity factor for crack 1 at the close (right) tip, ($s_1 = a_1$)

$K_{I_{L1}}$: Mode I stress intensity factor for crack 1 at the far (left) tip, ($s_1 = -a_1$)

$K_{II_{L1}}$: Mode II stress intensity factor for crack 1 at the far (left) tip, ($s_2 = -a_2$)

$K_{I_{L2}}$: Mode I stress intensity factor for crack 2 at the close (left) tip, ($s_2 = -a_2$)

$K_{II_{L2}}$: Mode II stress intensity factor for crack 2 at the close (left) tip, ($s_2 = a_2$)

$K_{I_{R2}}$: Mode I stress intensity factor for crack 2 at the far (right) tip, ($s_2 = a_2$)

$K_{II_{R2}}$: Mode II stress intensity factor for crack 2 at the far (right) tip, ($s_2 = a_2$)

Superdislocations

In this section the way to represent the interacting cracks by pairs of superdislocations will be presented. Later, in the results and discussion section, the accuracy of this representation will be analyzed on some sample cases. If the approach is valid, this means further analysis could be carried out in order to represent the complete stress field and stress intensity factors by simple algebraic expressions as done in [14], [18] and [19] for cylindrical cracks.

In order to find the parameters related to superdislocations, crack problem is solved and dislocation density distribution is obtained first, because at this stage the applicability of the technique is analyzed. Once this was done then investigation of the methods for direct closed form representations of the locations and strengths of the

superdislocations would further be investigated separately. When the density distributions are known the strengths of superdislocations can be found using the following integration

$$B_{jk} = \int_0^{S_0} b_j(s)ds \tag{17}$$

and the positions of superdislocations are defined by the first moment of densities as

$$S_{jk} = \frac{1}{B_{jk}} \int_0^{S_0} b_j(s)s\, ds \tag{18}$$

where S_0 indicates the point along the crack line where dislocation density changes sign and j=1,..4, k=L(left), R(right). This representation is slightly different than the previously presented one in [18]. The upper integration boundary is chosen to be the points where the dislocation density changes sign allowing more than one superdislocation in either side of the axis while in previous definition the boundary was always 1. The current definition of superdislocation strengths may allow a better representation of cracks. When previous definitions were kept, the model might give slightly less accurate results. The components of stresses at any given point in the domain are obtained from the expressions of σ_{XX}, σ_{YY}, σ_{XY} which are given in Appendix B. The only modification in these equations is to remove the integration sign and use B_{jk} for dislocation densities. The origin of global reference coordinate is chosen at the center of crack 1 and X to be parallel to crack 1.

The well known Peach-Koehler formula [15] can be employed to find the force on any dislocation between the two cracks as follows

$$F_k = -\varepsilon_{ijk}\xi_i\sigma_{jm}b_m \tag{19}$$

where b_m is the component of the Burgers vector of a given dislocation, ξ_i is the unit vector parallel to the dislocation line, σ_{jm} is stress tensor at that certain location. Using the above formulation it is possible to analyze equilibrium positions and motion of available dislocations in the domain where multiple cracks interact. Since the stresses can be obtained in closed form replacing integration that includes b(s) by B_{jk} in the stress expressions of Appendix B the force on a dislocation or interaction energy can also be obtained in closed form.

Similarity between the stress fields of the superdislocations and cracks would further imply that interaction energy between the superdislocations, which is related to

interaction force, can be used to represent the energy release rate in cracks. This aspect is useful in obtaining a closed form representation for the stress intensity factors, because the stress intensity factors are connected to energy release rate (G) or J integral by the following expression

$$G = \frac{K^2}{2\mu'} \tag{20}$$

where $\mu' = \mu/(1-\nu)$ for plane strain, and $\mu' = (1+\nu)$ for plane stress. An approximate form of K_I and K_{II} at the tips of each interacting crack will be expressed in algebraic form using B_{jk}'s, (i.e. the strengths of superdislocations where j=1,2,3,4 and k=L,R) as follows

$$\begin{aligned} K_{I_{R1}} = 2\{&[\sigma_{yy}(B_{1L},S_{1L}) + \sigma_{yy}(B_{2L},S_{2L}) + \sigma_{2R},S_{2R}) + \sigma_{yy}(B_{3L},S_3L) \\ &+ \sigma_{yy}(B_{3R},S_{3R}) + \sigma_{yy}(B_{4L},S_{4L}) + \sigma_{yy}(B_{4R},S_{4R}) + \sigma_o]B_{1R}\}^{1/2} \end{aligned} \tag{21}$$

as multiplying factor. B_{jk}'s are obtained for only sample cases in the present study, because showing the validity of the approximation is the primary purpose at this point. Expressing the positions and strengths of superdislocations representing cracks of different orientations and positions as functions of these parameters could be achieved in follow up studies which would result closed form stress intensity factors.

Results and Discussion

There are different parameters involved in the problem such as the relative lengths, positions and orientations of the cracks and applied loading conditions. The stress intensity factors, dislocation density distributions, crack opening displacements and extended stress field are obtained by changing each one of these parameters. Since the produced data and graphs are too many to present here, only the ones clearly showing the aspects which have been untouched, ignored or not commented by previous researchers and the significance of the new feature, superdislocation, will be emphasized.

The unit length is considered as a_1 which is the half length of crack 1. Determination of the effect of different parameters on the stress intensity factors and the stress distributions has been the main subject of this and other studies on crack interactions. All aspects at every crack tip must be considered in the analysis. Concentrating only on micro-crack(s) ahead of a main crack to decide about crack shielding zones could be misleading. Because while shielding occurs at the close tip the stress intensity factor could still be increased at the far tip mainly as a result of

finiteness of the main crack. This point was not mentioned or emphasized in previous articles when the shielding and amplification zones were found making their conclusions invalid for finite crack interactions.

Contour lines of normalized mode I stress intensity factors at the tip of one crack is plotted for different positions of the center of the other crack ahead of that tip (e.g. different positions of crack 2 around crack 1). Among these contours the one whose value is 1 marks the border between shielding and amplification zones showing the so called neutral positions of crack 2 where the polar angles of these neutral positions are named as neutral angles for considered polar radius. Discussions on this concept are included in previous studies [1-7]. The similar contour lines are plotted for the two finite cracks in this study to highlight some of the points and clarify them by comparing with the previous studies. Figs. 2 and 3 show some of them. The center of the coordinates is chosen at the right hand side tip of crack 1. This corresponds to the main crack tip of the previous studies in the case of semi-infinite crack which is the same as taking crack 1 much bigger than crack 2. As pointed out in Fig. 2, for the equal length cracks, determining a single contour line marking the shielding and amplification zones may be misleading. When both ends of crack 1 are considered different positions of crack 2 may cause shielding at one end while it still causes amplification at the other one. If the shielding is observable at both ends for certain positions this can be named as absolute shielding. The word "absolute shielding" implies $K_I < 1$ at both ends.

Figure 2 is plotted for two parallel cracks with equal lengths and absolute shielding and amplification zones are defined when the normalized mode I stress intensity factor for crack 1 is considered at both ends. When the length ratio $\rho = a_2/a_1$ changes contours will also change. The smaller ratio reduces the absolute shielding zone. For a ratio of ρ=0.1, there will be no absolute shielding zone. On the other hand the effect of crack 2 on the far tip will be insignificant. Considering the results related only one end of the bigger crack when ρ is small, ρ=0.1 for instance, would be satisfactory for the analysis of the shielding zones around the tip of a semi-infinite main crack. It can be concluded that when the sizes of two interacting cracks are comparable, a reduction on the critical stress intensity factors for both crack ends can be observed, but if they are too different such as macro-micro crack interaction, an absolute reduction in the critical stress intensity factor can not be expected. Since there are two contours for the normalized stress intensity factor corresponding unity, we can talk about two sets of neutral angles and neutral contour lines instead of one for comparable crack sizes. This makes the conclusions drawn based on semi-infinite crack related to the shielding and amplification zones invalid when finite crack lengths are considered. Highlighting this point that has not been specifically mentioned in the previous studies is one of the objectives of this study.

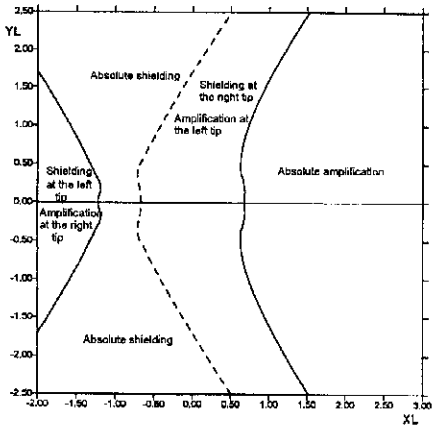

Fig. 2. Shielding and amplification zones due to an equal length parallel crack ahead of an existing crack. Mode I stress intensity factor $K_{I_{R1}}$ is considered only. The loading is perpendicular to crack 1.

When nondimensionalized coordinates are scaled by ρ the contours of $K_{I_{R1}}$ look similar for different ratios, however they are not the same oppose to the claims in [3], [6] and some other previous studies. The contours of $K_{I_{R1}}$ are presented for ρ=1 and 0.1 together in Fig. 3 for parallel cracks to show the difference between them. Extensive investigations were made into the effect of ρ. Since the main character of the curves do not change very much for close tips, presenting only the results showing $K_{I_{R1}}$ in Fig. 3 considered as sufficient in emphasizing that the contours are not the same for different ρ. This is another point that has not been explained in the previous studies such as [3],[5] and [6]. The parameter used in these referred articles is d/a which is the ratio between the distance from the right tip of crack 1 to the center of crack 2 (d), and the length of the second crack (a) corresponding to crack 2 in our case.

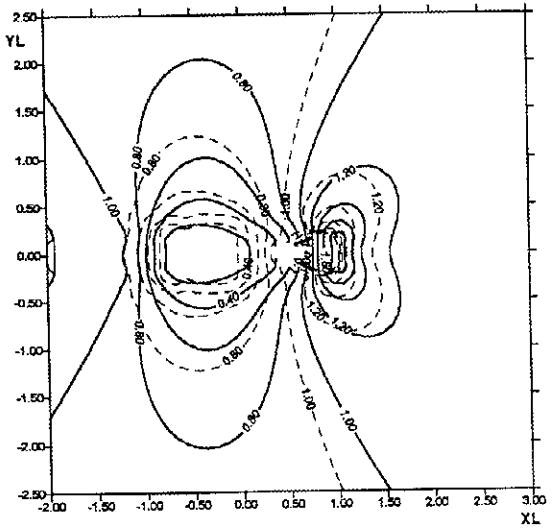

Fig. 3. Comparison of $K_{I_{R1}}$ for $\rho = 1$ (solid lines) for $\rho = 0.1$ (dotted lines) in the case of parallel cracks.

As seen in Table 1. we named that ratio as d/a_2 and tabulated values of $K_{I_{R1}}$ for different ρ and the same d/a. As clearly seen in the table and in Fig. 3 as well, the values differ for different ρ even if d/a did not change, while it is claimed in previous references that $K_{I_{R1}}$ values do not change for the same d/a_2 which is correct only when crack 1 is semi-infinite or practically ρ is very small. This reveals another important point that changes the conclusions of the previous studies. Although is not presented here, it should be clear that stress intensity factors $K_{I_{L1}}$ and $K_{II_{L1}}$ on the far tip will differ completely for different ρ.

Table 1. Comparison of the values of $K_{I_{R1}}$ for a configuration of collinear cracks

				Present study			
				Crack model		Superdislocation	
d/a_2	Gong and Horii [2]	Rose [1] (exact)	Lam et. al. [3]	ρ=0.1	ρ=1.	ρ=0.1	ρ=1
1.1	1.329	1.652	1.642	1.623	1.787	1.357	1.582
1.3	1.211	1.274	1.279	1.276	1.356	1.259	1.313
1.5	1.147	1.167	1.173	1.172	1.228	1.219	1.214
2	1.074	1.076	1.081	1.081	1.111	1.174	1.113

Thus the word shielding in previous papers have a meaning for only one end, and conclusions based on this would be meaningful when ρ is very small (i.e. semi-infinite crack and micro-crack). For instance the results obtained by taking ρ=0.1 agrees very well with the previous macro-micro-crack interaction cases as seen in Table 1. Position of crack 2 is not taken very close to crack 1 mainly due to numerical problems in the solution and the contours are extrapolated for these points. This is also justified physically. Because when position of crack 2 is very close to crack 1 it mostly results in crack coalescence and corresponding locations do not need to be taken into account as also noted in previous studies [3;16].

The contours for $K_{I_{R1}}, K_{II_{R1}}, K_{I_{L2}}$ and $K_{II_{L2}}$ when $\alpha_c = 45^\circ$ and $\rho = 1$ are plotted in Figs. 4a-4d in order to show the effect of the relative orientations of the cracks and mixed mode effect due to interaction. It is also noticeable after comparing with Fig. 3 that the change caused by the inclined crack is less severe than that of the parallel crack.

Figure 4 shows the contour lines of constant stress intensity factors when crack 2 is inclined 30 degrees. Since the case of intersecting cracks needs slightly different approach it is not included in the formulation. The contour lines are not drawn at the positions of the center of crack 2 that correspond to intersecting cracks and that region is left blank in Figs. 4a-4d.

Figure 4b shows the contours of $K_{II_{R1}}$. The values are very small and the only reason for mode II is the interaction effect of crack 2. Although the character of the contours are similar in general the values of $K_{II_{R1}}$ are slightly higher in the case of parallel cracks of which are not plotted here. This means crack 2 inclination reduces mode II effect on crack 1. The contour line showing zero corresponds to neutral positions when only mode II is considered.

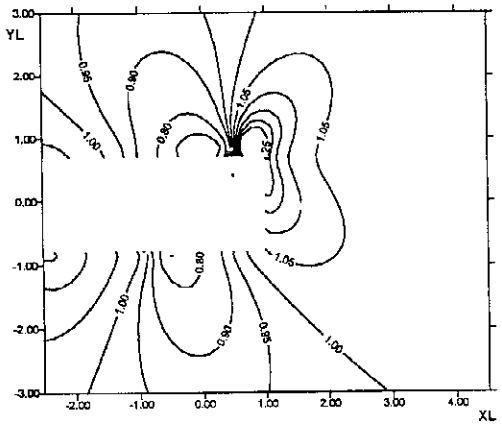

Fig. 4a. Contour lines for $K_{I_{RI}}$ at $\alpha_c = 45°$, $\rho = 1$.

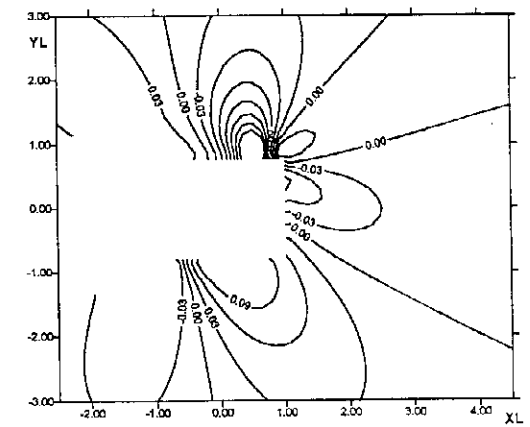

Fig. 4b. Contour lines for $K_{II_{RI}}$ at $\alpha_c = 45°$, $\rho = 1$.

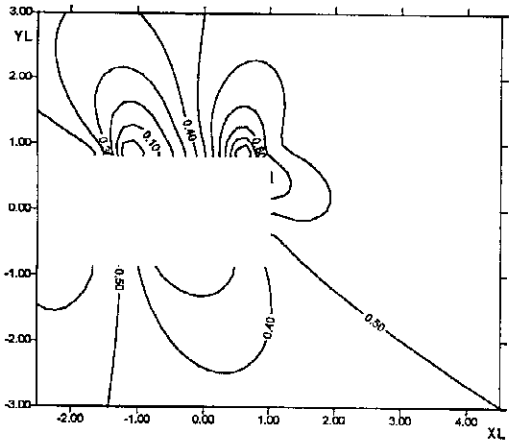

Fig. 4c. Contour lines for $K_{I_{L2}}$ at $\alpha_c = 45°$, $\rho = 1$.

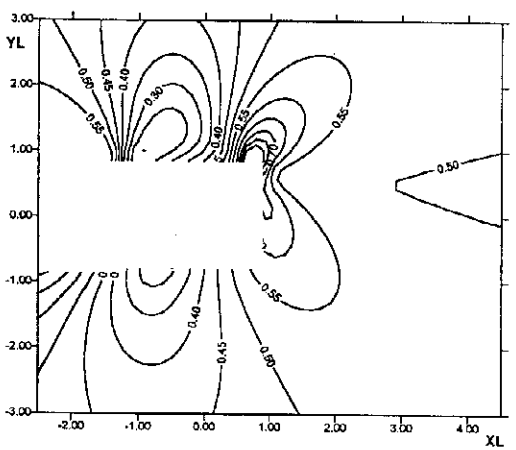

Fig. 4d. Contour lines for $K_{II_{L2}}$ at $\alpha_c = 45°$, $\rho = 1$.

The contours of $K_{I_{L2}}$ and $K_{II_{L2}}$ are presented in Figs. 4c and 4d respectively. The coordinates are defined the same way as in 4a and 4b. Since the inclination of crack 2 is 45°, equal constant mode I and mode II effects are expected if it were the only crack in the domain. However interaction disturbs this equality both in magnitude and distribution. The stress intensity factors are normalized by K_1, therefore the value of 0.5 in Figs. 4c and 4d marks the border between the amplification and shielding.

Figures 4a-4d give some idea about the effect of crack 2 inclination in all around crack 1 however this is just for a certain angle and in order to see the effect of complete range of inclination angles from 0 to 180 degrees Figs. 5a-5d are presented. Contours are plotted by changing α_c and Y_L. The value of $X_L = 1.1$ is fixed. This value is chosen because high amplification is expected there and it also prevents crack penetration. Expected symmetry in Figs. 5a and b is noticeable. In Fig. 5a amplification is observable on $K_{I_{R1}}$ through wide range of values of Y_L and α_c except very high values of Y_L, i.e., crack 2 far away from crack 1 and when α_c is close to 90 degree where it is practically ineffective in the given loading conditions. When the cracks are almost parallel and Y_L is smaller, the highest amplification is observed. A similar behavior is observed for different crack length ratios. Figure 5b also reveals a skew-symmetric contour distribution for $K_{II_{R1}}$ and when α_c is increased mode II effect diminishes. When crack 2 parallel or nearly parallel to crack 1 the changes in Y_L create sharp changes in $K_{I_{R1}}$ and in fact it reaches its maximum at some Y_L values while it vanishes when $Y_L = 0$. Observing the changes in not only mode I but also mode II stress intensity factor and analyzing its behavior is considered to be important and it has not been reported in detail previously except the discussion in a recent study [20]. There happens to be a mode II effect in crack 1 while that effect would have been 0 if it were the only crack. Therefore for a mode II sensitive material this point must be taken into consideration.

When crack 2 is inclined, the uniaxial loading will cause mixed mode conditions on it, even if it is the only crack. The orientation angle α_c will be the most important factor on the stress intensity factors of crack 2. This aspect is observable in Figs. 5c and 5d. The effect of Y_L is not very significant for $\rho=1$ while it is more noticeable for $\rho=0.1$ especially for smaller values of Y_L. The definition of stress intensity factors involves the half crack length and normalizing factor K_1 always include the length of crack 1 in the entire process. Therefore when the stress intensity factor values for crack 2 at different crack lengths are evaluated the effect of the normalization must be considered.

Figures 5a and 5b are plotted for the case of $\rho=1$ only. Because the effect of different crack lengths (different ρ) is already presented in Fig. 3 and it gives some idea about the order of effect. However for crack 2 this effect need to be presented and this has been done by plotting $\rho=1$ and $\rho=0.1$ cases together in Figs. 5c and 5d.

The results related to superdislocation modeling are presented in Figs. 6 and 7. First, the stress contours for two interacting cracks with the same lengths are presented in Figs. 6a-c by specifying the position and orientation of crack 2 as $X_L=1.5$, $Y_L=0$ and $\alpha_c = 30°$. There is no specific reason for choosing these parameters except to have a case which includes all modes in both cracks. Any other position could have been chosen as well. Since the purpose is to compare the stress fields of the exact solution of interacting cracks and their superdislocation equivalent, one case is thought to be sufficient to have some idea about the order of accuracy of the superdislocation representation.

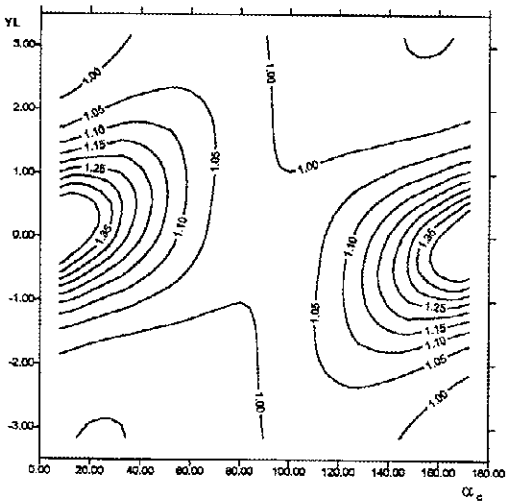

Fig. 5a. Contour lines for $K_{I_{R1}}$ at $X_L = 1.1$ $\rho = 1$, Y_L vs. α_c.

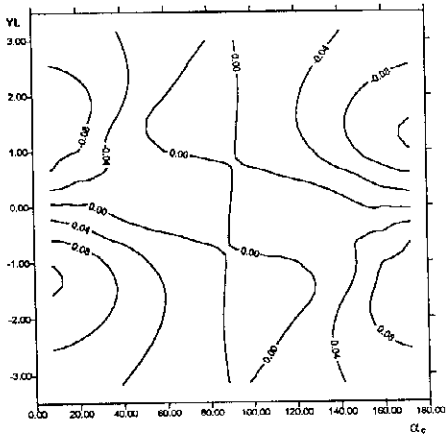

Fig. 5b. Contour lines for $K_{II_{R1}}$ at $X_L = 1.1$ $\rho = 1$, Y_L vs. α_c.

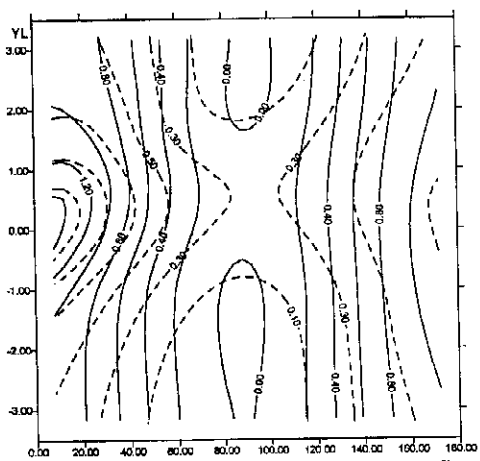

Fig. 5c. Contour lines for $K_{II_{L2}}$ at $X_L = 1.1$ $\rho = 1$, Y_L vs. α_c.
Solids lines: $\rho = 1$.,dotted lines: $\rho = 0.1$.

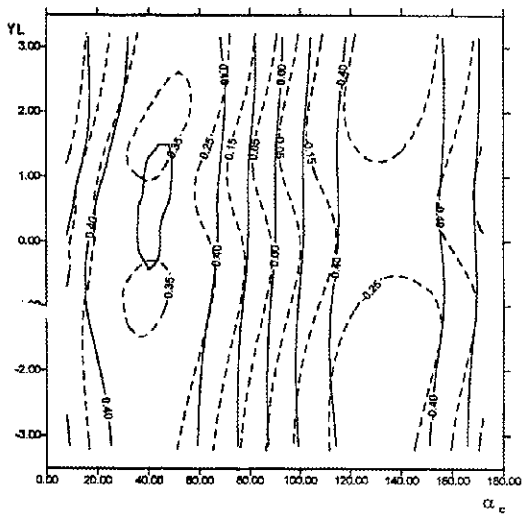

Fig. 5d. Contour lines for $K_{II_{L2}}$ at $X_L = 1.1$ $\rho = 1$, Y_L vs. α_c.
Solid lines: $\rho = 1.$, dotted lines: $\rho = 0.1$.

For the given position and orientation of cracks the strengths and positions of superdislocations which could represent the two cracks are given in Table 2 where L and R indicates left and right hand sides of cracks. Stress contours for σ_{xx}, σ_{yy} and σ_{xy} are plotted for two interacting cracks and their superdislocation equivalent using above numbers. The stress expressions derived form the basic formulation in [15] are given in the Appendix B. These expressions are used in the stress calculations. As seen in Figs. 6a - 6b stress contours of both cases are very similar especially for the extended stress field. This proves that extended stress field of interacting cracks can be approximately represented by the stress field of their superdislocation equivalents. However, the stress values near the crack tip region are not expected to be modeled very accurately by the superdislocation representation and this aspect is observable in the presented contours. Nevertheless the close similarity which is observed in the extended fields implies that superdislocations can replace crack especially if one considers the effect of the stress field on movable dislocation in the domain. Moreover by calculating interaction energies and forces, even stress intensity factors can be approximated by using the stress field of the superdislocations as shown in [19].

Table 2. The values of strengths and locations of the superdislocations

Strength		Location	
B_{1_L}	0.3492	S_{1_L}	-0.7765
B_{1_R}	-0.3492	S_{1_R}	0.8048
B_{2_L}	-0.0159	S_{2_L}	-0.6881
B_{2_R}	-0.0016	S_{2_R}	0.1476
	0.2760		0.1476
B_{3_L}	0.2760	S_{3_L}	-0.8166
B_{3_R}	-0.2760	S_{3_R}	0.7687
B_{4_L}	0.1386	S_{4_L}	-0.7968
B_{4_R}	-0.1386	S_{4_R}	0.7896

The accuracy of this representation has to be investigated. As an initial step two cases are considered in Figs. 7a and 7b. First, the location of the center of crack 2 is right ahead of crack 1 (Y_L=0) and second is above crack 1 (Y_L=1). Crack 2 is moved to different horizontal positions and also is rotated from 0 to 90 degree orientations. Fig. 7a compares the values of $K_{I_{R1}}$, which is the most interesting parameter in general, at Y_L=0. and X_L=1.1, 1.3, 1.5 obtained from exact solution and superdislocation representations. Fig. 7b does the same thing when crack 2 is at Y_L=1 and X_L=1.1, 1.5, 1.7. As can be observed in the above figures the superdislocation representation models the behavior of $K_{I_{R1}}$ very well qualitatively. The same trend is expected in the other stress intensity factors as well. Although some small percentage error is observable in quantitative manner, it is in acceptable limits. The main purpose here is to give an idea about the performance of the superdislocation model. The detailed analysis of the exact accuracy for different positions, orientations and length ratios of the cracks and following approximate analytical expressions for the stress fields and stress intensity factors can be the subject of another separate detailed study. At this point the present results suggest that since the extended stress fields of cracks and superdislocations are similar, analysis of the behavior of some dislocations or other defects and their motion in the presence of interacting cracks can be performed more conveniently by substituting their superdislocation equivalent. The convenience is basically due to the closed form stress expressions of the superdislocations. This in turn could be helpful in the analysis of plastic field around the cracks and in estimating the crack kinking and growth directions using different crack propagation criteria. Closed form force and energy relations between the interacting dislocations will be easier to produce resulting closed form representations of stress intensity factors when the positions and strengths of superdislocations estimated once. The presented results in Figs. 6 and 7 may not be enough to have a solid conclusion about the accuracy of the superdislocation representation quantitatively, however they suggest that this representation is promising and can model at least the interacting cracks qualitatively.

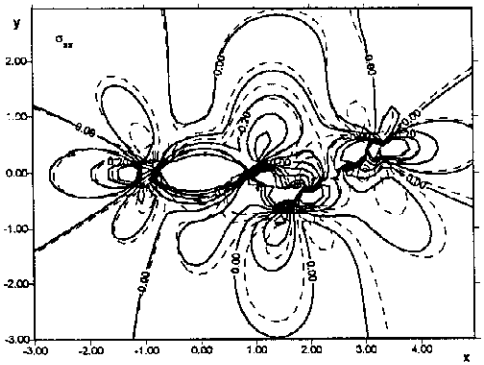

Fig. 6a. Comparison of the contour lines for stresses σ_{xx} due to interacting cracks (solid lines) and superdislocation representation (dotted lines) for the specific case of X_L=1.5, Y_L=0., ρ=1, α_c=30°.

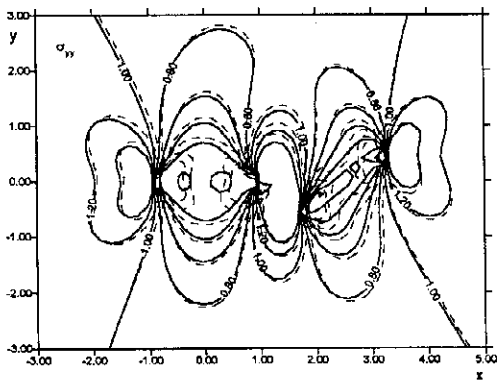

Fig. 6b. Comparison of the contour lines for stresses σ_{yy} due to interacting cracks (solid lines) and superdislocation representation (dotted lines) for the specific case of X_L=1.5, Y_L=0., ρ=1, α_c=30°.

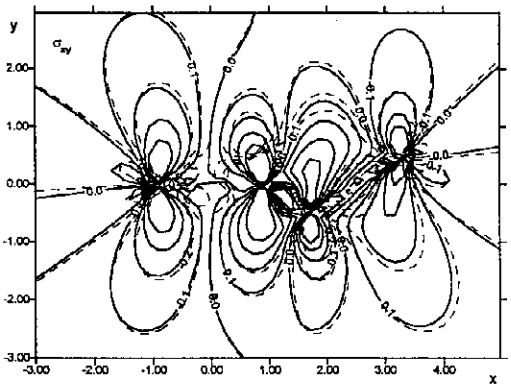

Fig. 6c. Comparison of the contour lines for stresses σ_{xy} due to interacting cracks (solid lines) and superdislocation representation (dotted lines) for the specific case of X_L=1.5, Y_L=0., ρ=1, α_c=30°.

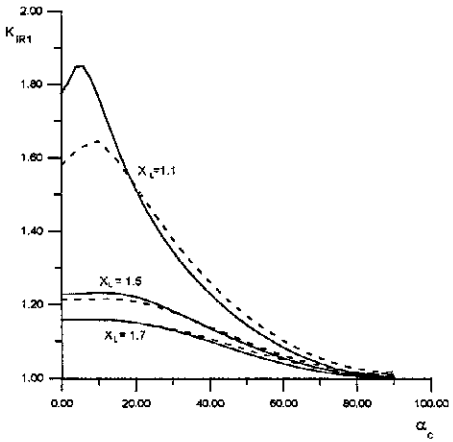

Fig. 7a. Comparison of the K_{I_1} found by the exact formulation and superdislocation representation in the case of equal length cracks. Dotted lines show superdislocation results. Crack 2 with different orientations at positions X_L=1.1,1.5,1.7, Y_L=0.

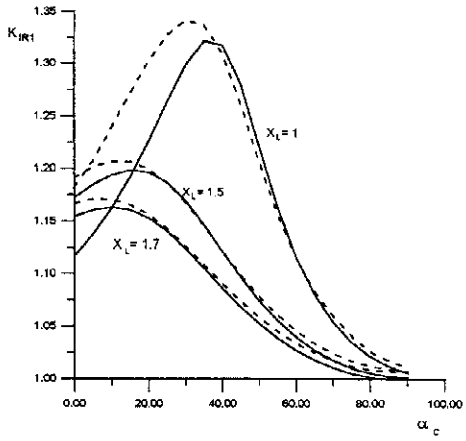

Fig. 7b. Comparison of the $K_{I_{R1}}$ found by the exact formulation and superdislocation representation in the case of equal length cracks. Dotted lines show superdislocation results. Crack 2 with different orientations at positions X_L=1, 1.5, 1.7, Y_L=1.

Conclusions

By using well developed dislocation density modeling in the analysis of interacting finite cracks the following basic conclusions can be reached.

Shielding and amplification zones must be decided by considering both ends of the cracks.

Demarcation line between the shielding and amplification zones and corresponding neutral angle as well as all the lines showing constant stress intensity factor contours depend on the relative crack sizes. A single neutral angle cannot be claimed for a different relative crack lengths.

Interaction causes a mode II effect even in the case of pure mode I generating loads. Although this effect is small it must be considered in the analysis. Moreover as pointed out in [20] whenever the critical conditions defined using energy release rate mixed mode effect will have a contribution on it and this in turn will effect the definition of neutral lines and angles.

Effect of crack inclination must be analyzed by considering both ends of all cracks and different crack length ratios.

Cracks can be modeled by superdislocations. This model is accurate especially when the extended stress field is considered. By using this representation the stress field of interacting cracks represented in approximate analytical form after finding out the strengths and locations of equivalent superdislocations.

The stress field expressions can be used to analyze the forces on dislocations. This feature is useful especially in investigating dislocation motion in the domain.

Using the concept of force on a dislocation and its relation with the energy release rate, stress intensity factors can approximately be defined based on superdislocation strengths and positions. This approximation is close enough as depicted in Figs. 7a and 7b. Quantitative assessment of the accuracy of the present approximation need to be analyzed separately in great detail.

References

[1] Rose, L.R.F. "Microcrack Interaction with a Main Crack." *Int. J. Frac.*, 31 (1986), 233-242.

[2] Gong, S.X. and Horii, H. "General Solution to the Problem of Microcracks Near the Tip of a Main Crack." *J. Mech. Phys. Solids*, 37 (1989), 27-46.

[3] Lam, K.Y., Wen, C. and Tao, Z. "Interaction between Microcracks and a Main Crack in a Semi-infinite Medium." *Eng. Frac. Mech.*, 44, No.5 (1993), 753-761.

[4] Wen, C. and Lam, K.Y. "Effect of Multiflat Inclusions on Stress Intensity factor of a Semi-infinite Crack." *Eng. Frac. Mech.*, 47, No.2 (1994), 157-168.

[5] Rubinstein, A.A. "Macrocrack-Microdefect Interaction." *J. Appl. Mech.*, 53 (1986), 505-510.

[6] Gong, S.X. and Meguid, S.A."Microdefect Interacting with a Main Crack: General Treatment." *Int. J. Mech. Sci.*, 34, No.12 (1992), 933-945.

[7] Gong, S.X. "Microcrack Interaction with a Finite Main Crack: An Exact Formulation." *Int. J. Frac.*, 66 (1994), R51-R56.

[8] Hutchinson, J.W. "Crack Tip Shielding by Micro-cracking in Brittle Solids." *Acta Metal*, 35 (1987), 1605-1619.

[9] Ortiz, M. "Continuum Theory of Crack Shielding in Ceramics." *J. Appl. Mech.*, 54 (1987), 54-59.

[10] Laures, J.P. and Kachanov, M. "Three-dimensional Interactions of a Crack Front with Arrays of Penny Shaped Micro-cracks." *Int. J. Frac.*, V.48 (1991), 255-261.

[11] Wang, X-M, Gao, S. and Chen, Y-H. "Further Investigation for the Macro-microcrack Interaction -I: In the Infinite Isotropic Body." *Int. J. of Solids and Structures*, 33, No.27 (1996), 4051-4064.

[12] Tamuzs, V., Petrova, V. and Romalis, N. "Plane Problem of Macro-Microcrack Interaction with Taking Account of Crack Closure." *Eng. Frac. Mech.*, 5, No.6 (1996), 957-967.

[13] Brencich, A. and Carpinteri, A. "Interaction of a Main Crack with Ordered Distributions of Microcracks: A Numerical Technique by Displacement Discontinuity BEs." *Int. J. Frac.*, 76, No. 4 (1996), 373-379.

[14] Zbib, H.M. and Close, S. "The Stress Intensity Factors and Interaction between Cylindrical Cracks in Fiber-Matrix Composites." *Damage and Interfacial Debonding in Composites*. G.Z. Voyiadjis and D.H. Allen (Eds.), Elsevier, 1995.

[15] Hirth, J.P. and Lothe, J. "*Theory of Dislocations*." 2nd ed., New York: Wiley, 1982.

[16] Hoagland, R.G. and Embury, J.D. "A Treatment of Inelastic Deformation around a Crack Tip due to Microcracking." *J. Am. Ceram. Soc.*, 63 (1960), 404-410.
[17] Erdogan, F. and Gupta, G. "On the Numerical Solution of Singular Integral Equations." *Quart. Appl. Math.*, 30 (1972), 525-534.
[18] Demir, I., Hirth, J.P. and Zbib, H.M. "Extended Stress Field around Cylindrical Crack Using the Theory of Dislocation Pile-ups." *Int. J. Eng. Sci.*, 30 (1992), 829-845.
[19] Zbib, H.M., Hirth, J.P. and Demir, I. "Stress Intensity Factors in Cylindrical Cracks." *Int. J. Eng. Sci.*, 33, No. 2 (1995), 247-253.
[20] Wang, X.-M., Gao, S. and Shen, Y.-P. "Discussion on the Neutral Angle of Macrocrack-microcrack Interaction.", *Eng. Frac. Mech.*, 54, No.4 (1996), 597-599.

Appendix A

The kernels in the integral equations are given as follows by referring Fig. A.

$$K_{13} = \frac{\cos\theta_2}{r_2} - \frac{\sin\theta_2}{r_2}\sin(2\gamma),$$

$$K_{14} = -\frac{\sin\theta_2}{r_2} - \frac{\cos\theta_2}{r_2}\sin(2\gamma),$$

$$K_{23} = \frac{\sin\theta_2}{r_2}\cos(2\gamma),$$

$$K_{24} = \frac{\cos\theta_2}{r_2}\cos(2\gamma),$$

$$K_{31} = \frac{\cos\theta_1}{r_1} - \frac{\sin\theta_1}{r_1}\sin(2\beta),$$

$$K_{32} = -\frac{\sin\theta_1}{r_1} - \frac{\cos\theta_1}{r_1}\sin(2\beta),$$

$$K_{41} = \frac{\sin\theta_1}{r_1}\cos(2\beta),$$

$$K_{42} = \frac{\cos\theta_1}{r_1}\cos(2\beta).$$

where

$$c = x_c^2 + y_c^2, \quad \theta_c = \tan^{-1}\left(\frac{y_c}{x_c}\right)$$

$$x_p = x_c + x_2\cos\alpha_c - s_1, \quad y_p = y_c + x_2\sin\alpha_c$$

$$r_1^2 = \sqrt{x_p^2 + y_p^2}, \quad \cos\theta_1 = \frac{x_p}{r_1}, \quad \sin\theta_1 = \frac{y_p}{r_1}$$

$$\beta = -(\theta_1 - \theta_c)$$

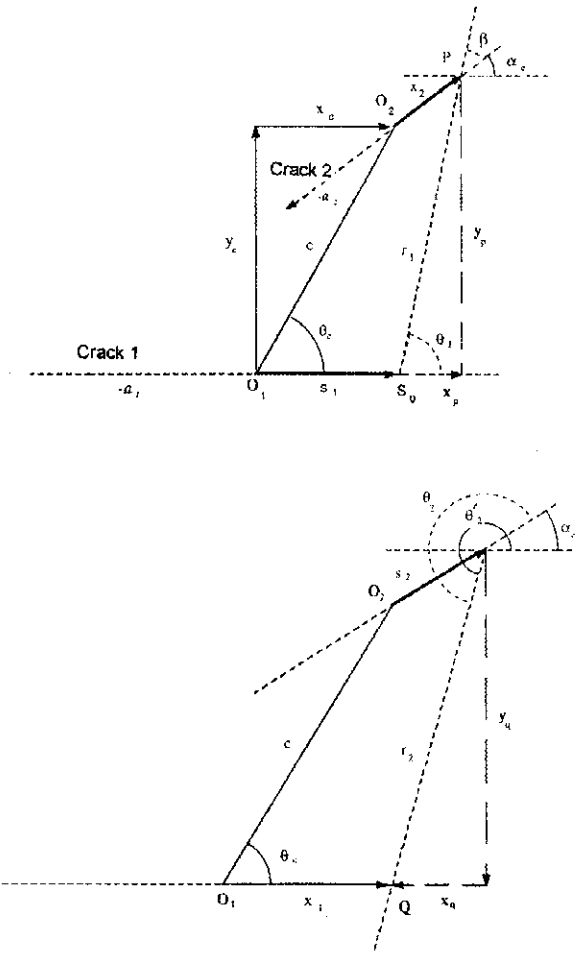

Fig. A. Parameters defining the relative positions of the points on each cracks.

$$x_q = -x_c - s_2 \cos\alpha_c + x_1, \quad y_q = -x_c - s_2 \sin\alpha_c$$

$$r_2^2 = \sqrt{x_q^2 + y_q^2}$$

$$\cos\theta_2' = \frac{x_q}{r_2}, \qquad \sin\theta_2' = \frac{y_q}{r_2}$$

$$\gamma = -\theta_2', \qquad \theta_2 = \theta_2' - \alpha_c$$

Appendix B

Stress expressions due to two cracks which are represented by dislocation density distributions are given as follows

$$\sigma_{XX} = -D\left[\int_{-1}^{1} b_1(s_1)\frac{x_{s1}\left[x_{s1}^2 - y_{s1}^2\right]}{\left(x_{s1}^2 + y_{s1}^2\right)}ds_1 + \int_{1}^{1} b_1(s_1)\frac{y_{s1}\left[y_{s1}^2 + 3x_{s1}^2\right]}{\left(x_{s1}^2 + y_{s1}^2\right)}ds_1\right]$$
$$- D\left[\int_{-1}^{1} b_3(s_2)\frac{x_{s2}\left[x_{s2}^2 - y_{s2}^2\right]}{\left(x_{s2}^2 + y_{s2}^2\right)}ds_2 + \int_{1}^{1} b_4'(s_2)\frac{y_{s2}\left[y_{s2}^2 - 3x_{s2}^2\right]}{\left(x_{s2}^2 + y_{s2}^2\right)}ds_2\right]$$

$$\sigma_{YY} = D\left[\int_{1}^{1} - b_1(s_1)\frac{x_{s1}\left[x_{s1}^2 + 3x_{s1}^2\right]}{\left(x_{s1}^2 + y_{s1}^2\right)^2}ds_1 + \int_{-1}^{1} b_2(s_1)\frac{y_{s1}\left[x_{s1}^2 - y_{s1}^2\right]}{\left(x_{s1}^2 + y_{s1}^2\right)^2}ds_1\right]$$
$$+ D\left[\int_{-1}^{1} - b_3'(s_2)\frac{x_{s2}\left[x_{s2}^2 + 3y_{s2}^2\right]}{\left(x_{s2}^2 + y_{s2}^2\right)^2}ds_2 + \int_{-1}^{1} b_4'(s_2)\frac{y_{s2}\left[x_{s2}^2 - y_{s2}^2\right]}{\left(x_{s2}^2 + y_{s2}^2\right)^2}ds_2\right]$$

$$\sigma_{XY} = D\left[\int_{-1}^{1} - b_1(s_1)\frac{y_{s1}\left[y_{s1}^2 - x_{s1}^2\right]}{\left(x_{s1}^2 + y_{s1}^2\right)^2}ds_1 + \int_{-1}^{1} b_2(s_1)\frac{x_{s1}\left[x_{s1}^2 - y_{s1}^2\right]}{\left(x_{s1}^2 + y_{s1}^2\right)^2}ds_1\right]$$
$$+ D\left[\int_{-1}^{1} - b_3'(s_2)\frac{y_{s2}\left[y_{s2}^2 - x_{s2}^2\right]}{\left(x_{s2}^2 + y_{s2}^2\right)^2}ds_2 + \int_{-1}^{1} b_4'(s_2)\frac{x_{s2}\left[x_{s2}^2 - y_{s2}^2\right]}{\left(x_{s2}^2 + y_{s2}^2\right)^2}ds_2\right]$$

where

$$b_3' = b_3 \cos\alpha_c + b_4 \sin\alpha_c$$

$$b_4' = b_3 \sin\alpha_c + b_4 \cos\alpha_c$$

$$D = \frac{2\mu}{\pi(\kappa+1)}$$

and dislocation density distribution $b_1(s)$, $b_2(s)$ represent crack 1 and $b_3(s)$, $b_4(s)$ represent crack 2. x_{s_1}, y_{s_1} and x_{s_2}, y_{s_2} are the cartesian coordinates of a point where the stresses are calculated. They are measured from a location on crack 1 (s_1) or crack 2 (s_2) respectively.

تبادل التأثير بين التشققات المحدودة

إسماعيل عمر ديمير

قسم الهندسة الميكانيكية ، كلية الهندسة ، جامعة الملك سعود ، ص . ب ٨٠٠ ،

الرياض ١١٤٢١ ، المملكة العربية السعودية

(استلم في ١٩٩٧/٣/١٦م ، وقبل للنشر في ١٩٩٨/٣/٩م)

ملخص البحث . تمت دراسة التشققات المحدودة التي تقع في نطاق مستوي وغير محدود ، ونؤثر عليها أحمال مستوية بعيدة .يعتمد الاشتقاق الرياضي على أساس النمذجة بواسطة توزيع كثافة الانخلاعات . يمثل الاشتقاق العام حالة تشققين متفاعلين وإيجاد النتيجة لهذه الحالة .

تمت دراسة أثر الوضع النسبي ، الاتجاهات ، وأطوال التشققات على شدة معامل الإجهاد ومجال الإجهاد لتوضيح بعض الظواهر التي لم تدرس في السابق مثل : اعتماد المناطق الغير متأثرة والزوايا المحايدة على الأطوال النسبية للتشققات وكذلك أثر الوضع النسبي للتشققات على الأنماط الفعّالة للتشقق .

وبالإضافة إلى تصحيح وإكمال بعض النقاط في الدراسات السابقة تمت دراسة إمكانية تطبيق نموذج الانخلاع الفائق على مسائل التشققات المتفاعلة . تم إتمام العمل الأساسي لتمثيل قوة بيتش – كوهلير على الانخلاع في مجال التشققات المتفاعلة . ثم تم توضيح التقارب الشديد بين مجال الإجهاد في حالة التشققات المتفاعلة والانخلاع الفائق المكافئ لها .

كذلك تم إيجاد معاملات شدة الإجهاد باستخدام الحل الصحيح ونموذج الانخلاع الفائق التقريبي وتمت مقارنتها وظهر التقارب الشديد بينها . توضح النتائج المقدمة لحالات بسيطة أن الانخلاعات الفائقة يمكن أن تمثل التشققات ، ولكن لكي يتم التقويم بدقة كافية ، فإنه يتطلب إجراء تحليلات أخرى متضمنة كل الاحتمالات .